VIP Electrochemistry

DOI: 10.1002/anie.201200226

Dynamic Electrochemistry in Flame Plasma Electrolyte**

*Atif Elahi, Toks Fowowe, and Daren J. Caruana**

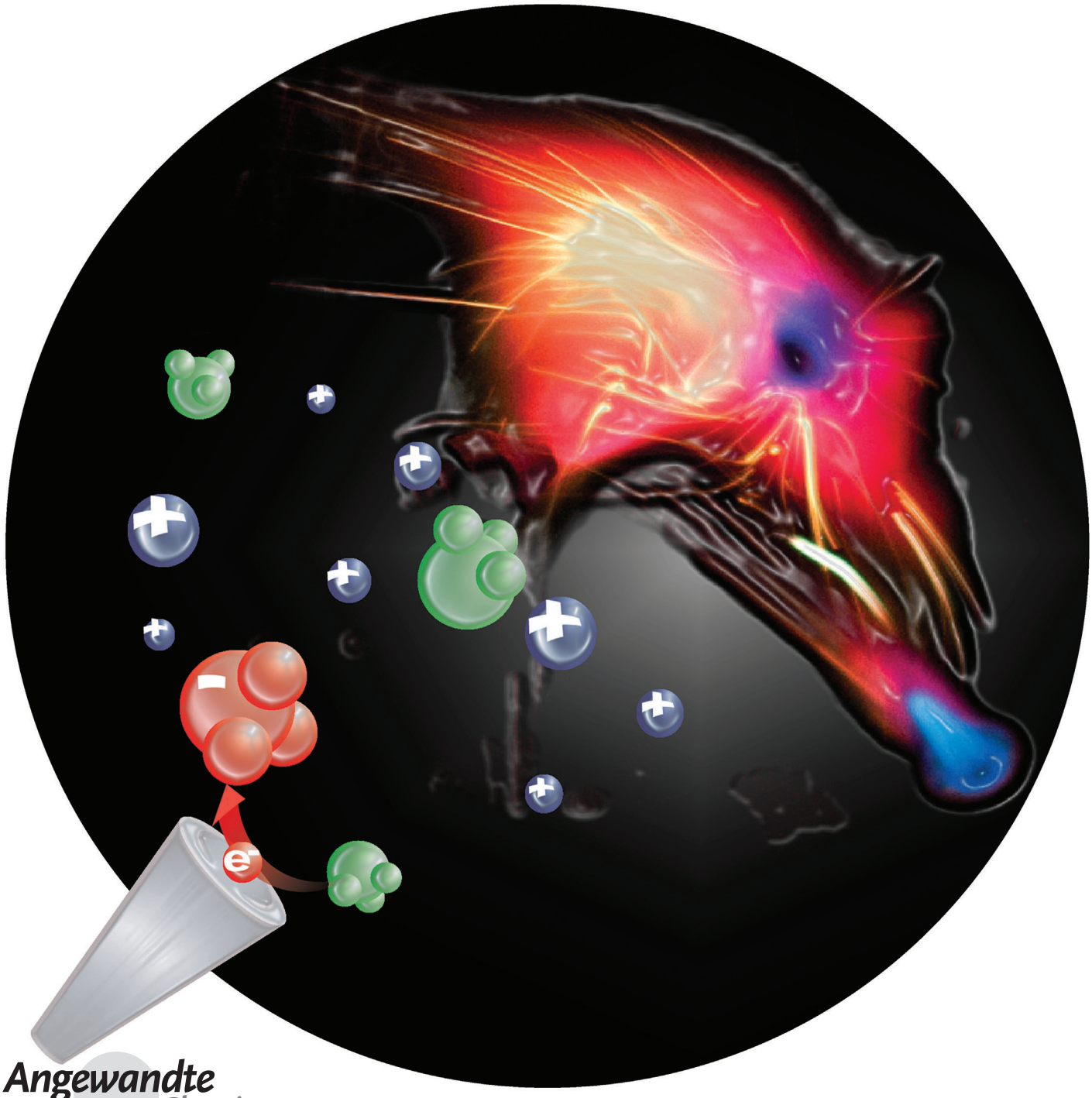

WILEY ONLINE LIBRARY

© 2012 Wiley-VCH Verlag GmbH & Co. KGaA, Weinheim

Electrochemistry underpins numerous commercially important processes ranging from energy conversion to sensors and coating deposition. A common and—so far—essential feature of all these processes involves a redox-active species dissolved in a liquid or solid, which serves to allow charge exchange between electrodes. Rather than being inert, the solvent is without exception redox-active at high potentials and thus restricts the breadth of observable reactions to a narrow potential window of approximately 4.5 to 6 V, as depicted in Figure 1 a.[1] Here we describe a new method of performing potentio-dynamic experiments in a liquid-free electrochemical system using a flame plasma as the electrolyte medium, to enable redox reactions beyond any solvent-defined potential limits, as shown in Figure 1 b.

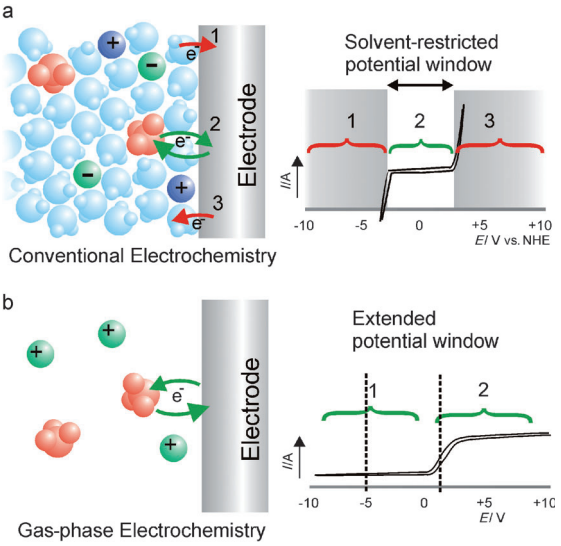

Figure 1. a) Redox reactions at a solid | liquid electrode and the corresponding solvent-limited voltammetry window within which redox reactions can be accessed. b) Solid | gas interfacial redox reactions and corresponding voltammetry (Langmuir probe characteristics) which is not limited by solvent. The region between the broken lines is investigated.

To date, redox reactions in the gas phase (electron attachment or detachment) are commonly studied using photoelectron spectroscopic or related techniques, in conjunction with mass spectrometry for analysis of products and/or reactants.[2] There are few examples using plasmas as media where redox reactions are investigated. Richmonds, Meiss, and Hickling investigated the charge-transfer processes at the plasma | liquid interface.[3] Vennekamp, Brettholle, and Ogumi described the use of non-thermal plasma for metal surface oxidation.[4] However, apart from experiments performed at especially designed interfaces,[5] there are no examples of voltammetry in the gas phase at a true solid | gas interface. Our new approach can help apply the well-established cornerstones of electrochemistry developed almost exclusively in liquids, to the new context of gas plasma.

Here we use flame plasma as electrolyte. In flames, negatively charged species are predominantly free electrons and positive species are complex ions.[6] While being relatively weak plasmas, flames have been chosen for this work over any other plasmas formed by discharge or microwave, because they are at close to thermal equilibrium ($T_{e^-} \approx T_m \approx T_{A^+}$)[7] and relatively easy to control in the laboratory. Furthermore, there is a large body of literature describing their physical and chemical properties[8] mostly from spectroscopic[9] and mass spectrometric[10] investigations. The flame medium here is the background electrolyte, serving no other role except to complete the circuit and transfer charge between electrodes.[11]

Stoichiometric and laminar-flow flame plasma was generated by igniting a premixed stream containing hydrogen, oxygen, and nitrogen using a specially designed burner.[12] As illustrated in Figure 2 a and b, the burner supports two separate premixed gas streams of equal size and matched velocity. The right flame section was doped with redox-active species and impinged directly onto a graphite-disc working electrode. By contrast, the left hand section of the flame was in contact with the reference electrode made of titanium wire and was undoped at all times. A platinum shield counter electrode completed the three-electrode setup (Figure 2 a and b). The current was recorded as a function of scanned potential applied to the working electrode as in conventional cyclic voltammetry, both in the forward and backward direction between the limits of $+1$ to -5 V versus Ti/TiO_2. Here we focus exclusively in the region more negative than the potential of zero charge, to ensure that the current measurement was independent of any free electron collection, and to ensure the stability of the reference electrode.[6b,13]

Successful electrochemical measurements at the solid | gas interface were demonstrated by doping the flame plasma with a metal oxide salt and recording distinct redox potentials. When nebulizing a solution of ammonium metatungstate hydrate [$(NH_4)_6H_2W_{12}O_{40}\cdot x\,H_2O$; herein referred to as tungsten oxide salt] into the right section of the flame, cyclic voltammogram scans showed four distinct peaks at i) $+0.13 \pm 0.03$, ii) -1.30 ± 0.08, iii) -3.04 ± 0.06, and iv) -4.35 ± 0.03 V in the negative direction (Figure 3 a). The peaks were present both in the positive and negative scan direction, at the same potential positions. In addition, the peaks were present on repetitive scanning in exactly the same positions (see Figure S3 in the Supporting Information). These current peaks most probably reflect redox reactions of metal oxide species. In one control experiment, peaks in the same position were also measured when the previous graphite was replaced with

[*] A. Elahi, Dr. T. Fowowe, Dr. D. J. Caruana
Department of Chemistry, University College London
Christopher Ingold Laboratory
20 Gordon St, London, WC1H 0AJ (UK)
E-mail: d.j.caruana@ucl.ac.uk

[**] The authors acknowledge the EPSRC (grant numbersEP/H049398/1 and GR/S45454/01), Royal Society of Chemistry, and The Leverhulme Trust for financial support. Dr. E. Hadzifejzovic, Dr. D. Sarantaridis, M. Li and Dr. J. R. Butler helped with the technical development of this work. Dr. S. Howorka is thanked for assistance with preparing the manuscript.

Supporting information for this article is available on the WWW under http://dx.doi.org/10.1002/anie.201200226.

 © 2012 Wiley-VCH Verlag GmbH & Co. KGaA, Weinheim

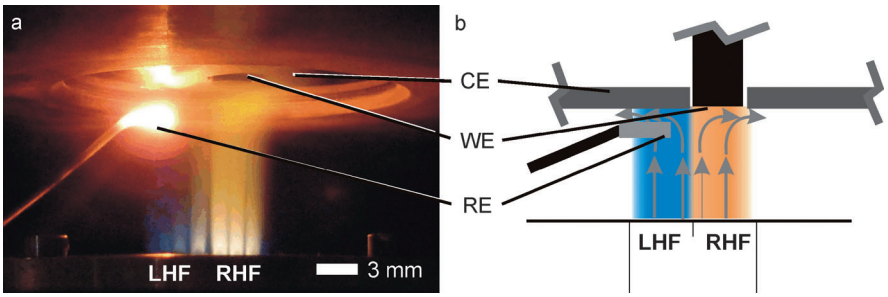

Figure 2. a) Photograph of the graphite carbon disc working electrode (WE) in contact with the right hand flame (RHF) doped with salts, titanium wire reference electrode (RE), positioned in the left hand flame (LHF), and platinum shield (CE). The scale bar is 3 mm. b) Schematic cross-section of the three electrodes in the flame, showing the position of the working electrode in a hole in the platinum electrode shield.

a platinum electrode, ruling out that the observed signals are an intrinsic property of the conducting electrode material. Furthermore, when the salts were removed from the flame the peaks disappeared, implying that the electrochemical response was from species in the flame and cannot stem from any material adsorbed at the working electrode (see the Supporting Information).

Cyclic voltammetry in a flame doped with metal oxides showed that the current peaks were dependent on 1) the identity of the metal oxide, 2) concentration, and 3) their stoichiometry of the metal salt, thereby supporting the Faradaic nature of the peak. Taking each point individually: 1) Replacing the tungsten oxide salt with ammonium heptamolybdate ($(NH_4)_6Mo_7O_{24}{\cdot}4H_2O$) yielded three principal peaks at $(+0.52\pm0.05)$, (-0.93 ± 0.02), and (-2.08 ± 0.03) V versus Ti/TiO_2 (Figure 3b) which are different to the tungsten salt (Figure 3a). Similarly, a third salt, ammonium metavanadate (NH_4VO_3), gave rise to two separate, weak peaks at (-1.04 ± 0.09) and (-2.23 ± 0.04) V versus Ti/TiO_2 (Figure 3c). 2) The peak heights as well as the integrated charge were linearly dependent on the concentration of the metal oxide salt in the solution used to dope the flame (Figure 4, tungsten oxide salt). Also in line with their Faradaic nature, 3) the varying peak heights for the three different complexes reflect the stoichiometric amount of metal atoms per mole of salt, when salt solutions of the same concentration were used. This was convincingly demonstrated using a fourth salt ($(NH_4)_2MoO_4$), which gave current peaks in exactly the same position as for the molybdenum salt ($(NH_4)_6Mo_7O_{24}{\cdot}4H_2O$) shown in Figure 3b. However, the ratio of charge for the peak at −2.08 V versus Ti/TiO_2 for these two salts was 6.8, matching well with the molybdenum oxide stoichiometry of the two salts which was 7, (see Figure S5 in the Supporting Information).

The most significant innovation that made these measurements possible was the formation of a reference electrode. Extensive assessment of several materials showed that titanium wire oxidized on the surface to produce a self-limiting layer of TiO_2, which is stable and forms a nonpolarizable electrode surface, and maintains a stable potential in the hydrogen flame.[14] When a platinum wire of similar dimensions was placed in the same position in the flame, peaks of a similar magnitude can be observed when tungsten salt was added in the flame, see Figure S2 in the Supporting Information. However, they occur randomly with no align-

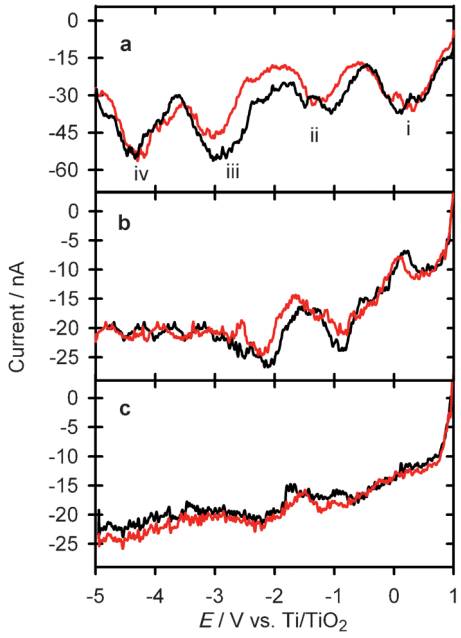

Figure 3. A flame electrolyte doped with three metal oxides yields specific cyclic voltammetry signals. Aqueous solutions containing 1×10^{-3} mol dm^{-3} a) $(NH_4)_6H_2W_{12}O_{40}$, b) $(NH_4)_6Mo_7O_{24}$, and c) NH_4VO_3 were nebulized in the right hand flame. Forward (black) and backward (red) scans were conducted at a rate of 1 V s^{-1}. The forward scan was started at 1 V. For further experimental details see the Supporting Information.

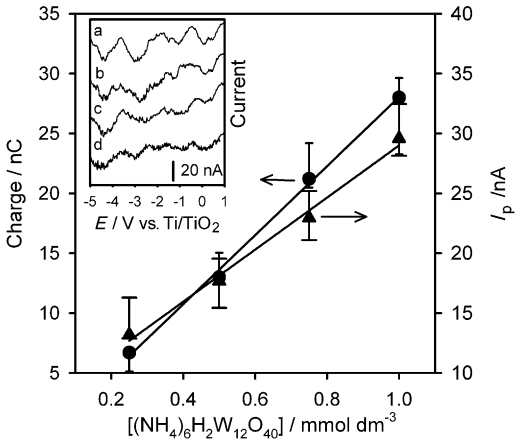

Figure 4. The dependence of height and integrated charge of peak (iii) at −3.037 V on the concentration of $(NH_4)_6H_2W_{12}O_{40}$ nebulized into the premixed gases of the RHF. The inset shows the forward scan with 1.0, 0.75, 0.5, and 0.25 mmol dm^{-3} labeled a, b, c, and d, respectively, of a tungsten oxide salt solution nebulized into the premixed gases.

© 2012 Wiley-VCH Verlag GmbH & Co. KGaA, Weinheim

ment with potential. This was expected as a platinum electrode is polarizable; even in these environments.[11a,15]

What is the physical or chemical origin of the peaks observed in the voltammograms? It is known that for both molybdenum and tungsten, the most thermodynamically stable oxides in flames are the trioxide species.[16] Given that our voltammetry experiment records reduction, it is very likely that the observed peaks correspond to the electrochemical process given in Equation (1) involving the distinct excited state of MO_3:

$$MO_3\ (gas) + e^-(metal) \rightarrow MO_3^-(gas) \quad (1)$$

In support of this interpretation, comparison of reduction potentials measured here for WO_3 and MoO_3 with the vertical electron detachment energies for MO_3^- showed excellent correlation.[2b] There was poor correlation with MO_4 or distinct excited state of MO_5 oxides. The plot shown of the reduction potentials against the vertical electron detachment energies (VDE) obtained from photoelectron spectroscopy (PES; Figure 5) presents further evidence that MO_3 is the molecular species being reduced at the gas | solid interface.

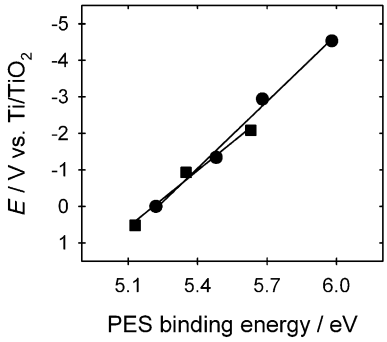

Figure 5. Comparison plot of the redox potential measured for peak potentials in the presence of $(NH_4)_6H_2W_{12}O_{40}$ and $(NH_4)_6MO_7O_{24}$ against the VDE measured by PES at 193 nm, against WO_3^- (●) and MoO_3^- (■), respectively. The PES data are taken from H. J. Zhai et al.[2b]

Interestingly, the presence of peaks for the reduction processes was unexpected. In this system with efficient aerodynamic mass transport of electroactive species to the electrode surface, a series of plateaus should be expected; not peaks. This may be rationalized by applying Gerischer's model based on distribution of energy states, considering the Fermi energy of the working electrode as it increases (more negative) by the application of an electrochemical potential.[1a]

Clearly electron transfer only occurs when there is a resonance between the Fermi energy, E_F, and the peak reduction potential, E_R, of the oxidized states in the gas phase (Figure 6). Once E_F increases above that of the lowest unoccupied molecular orbital (LUMO), electron transfer ceases as the reaction would be forbidden since in absence of any solvent, there are no channels to dissipate excess reaction

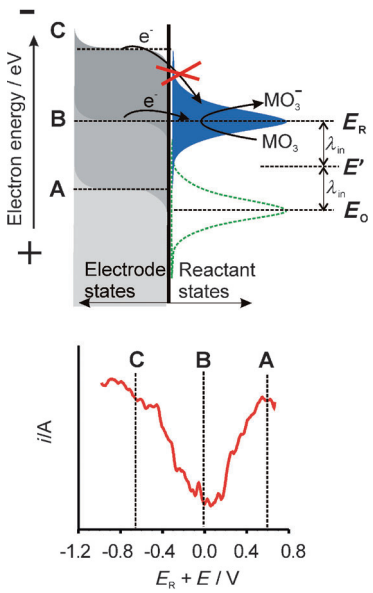

Figure 6. Energy states on an absolute scale, for the gas-phase reactant species (MO_3) and the electrons in the solid at different Fermi energies A, B, and C, showing that only when the Fermi energy is at B, electrons transfer to the reactant. At potentials lower (A) or higher (C) than B, electron transfer is forbidden.

energy. As a consequence the current decreases and a peak is observed.

Electrons below the Fermi edge in the working electrode are unavailable, despite an occupancy probability of close to unity; abstraction of electrons would lead to the formation of valence band holes. The current measured is proportional to the sum of the rate of electron transfer from metal to gas species over all the energy ranges given by the integral in Equation (2),[1a]

$$\text{Rate} = \nu A \int_{-\infty}^{\infty} P_o(E)N(E)dE \quad (2)$$

where ν and A are the frequency for the transition and area of the electrode, respectively. $P_o(E)$ is the transition probability for electron transfer to an oxidized state in the gas phase, which is proportional to the density of states $D_o(E)$, with a maximum at E_R, the peak reduction potential, shown in Figure 6. Figure 6 also shows the density of states for the reduced species, broken green line, with a maximum at the potential for oxidation, E_o. No oxidation processes were observed in our measurements, as any negatively charged species, from the reduction process, would be transported away from the negatively charged electrode very efficiently by electrostatic forces. The separation between E_R and E_o is twice the internal geometry reorganization factor λ_{in}, and the mid-point is the characteristic redox potential for this reaction, E'.

The density of states describes the most probable vibrational and electronic states within the potential wells. This will be a complex profile which is molecule specific and may be non-Gaussian. $N(E)$ is the density function of electrons in the metal and is the product of the density of states $\rho(E)$ and the

 © 2012 Wiley-VCH Verlag GmbH & Co. KGaA, Weinheim

occupancy probability $f(E)$, $N(E)=\rho(E)f(E)$. Where $f(E)$ is given by the Fermi–Dirac function in Equation (3),

$$f(E) = [1 + \exp(E - E_F/kT)]^{-1} \quad (3)$$

here k and T are the Boltzmann constant and temperature, respectively. E_F is the Fermi energy where the probability of finding an occupied state is 0.5. The width of this probability function spans an energy of approximately $4kT$, giving a Fermi edge with an energy range of 0.43 eV for an electrode surface temperature of 1236 K.

From this rationalization, the width at half height for the Faradaic reduction peaks should be greater than 0.43 eV, the magnitude depending on the width of the distribution in $D_o(E)$. This is consistent with the peak widths measured in the presence of WO_3 in the flame, Figure 3a, which range from 0.55 to 0.89 V for all the peaks between +1.00 and −5.00 V versus Ti/TiO_2. The reasoning presented here to account for the electrochemical signals measured in the gas phase, offers a framework of interpretation upon which a full mechanistic understanding can be based.

By adopting a seemingly uncomplicated experimental approach, a tool has been developed to study and control electron transfer events at the solid | gas interface. Our results have wide implications of academic and technological significance. Undoubtedly, and perhaps expectedly, there are significant departures from the analogous process in condensed phases. These departures present fruitful theoretical avenues for research to develop a microscopic theory to understanding electron transfer reactions at the solid | gas interface, perhaps mapped on to Marcus theory in absence of solvent. The scope of technological impact is extensive. Here we showed reduction/detection of metal oxides to the negative ion, as a model system. However, this work opens up the possibility of accessing redox reactions which are outside the potential limits set by the solvent in conventional liquid-phase electrochemistry.[17] Furthermore, this approach extends the use Langmuir probes, beyond conductivity measurements for the development of new plasma diagnostic tools.[18] Also quantitative gas-phase voltammetry may be developed, complementing analytical techniques such as atomic absorption, inductively coupled plasma, and fluorescence spectroscopies.[19]

Experimental Section

The flame mixture for all this work was the same for both sections; 1.6, 0.4, and 1.0 L min^{-1} for nitrogen, oxygen, and hydrogen, respectively. The total flow rate for the whole flame was 6.0 L min^{-1}. Pre-mixed hydrogen and oxygen gases are explosive and adequate safety precautions were taken. A Méker-type burner was used to create a stable homogenous flame with an adiabatic flame temperature of 2296 K.

A polished tip of a graphite rod (2.4 mm diameter) served as the working electrode, which was precisely positioned in a 3 mm hole in a platinum foil counter electrode. The clearance between the working electrode and the platinum foil counter electrode was important to define the surface area in contact with the flame, without the need for any insulating material. Once in the flame, the working electrode surface temperature was (1236 ± 15) K. The reference electrode was a 0.5 mm diameter length of a titanium wire. After conditioning the wire in the flame for 30 seconds the wire was then used as a reference electrode. The wire was placed in the left hand section of the flame, 1 mm away from the nearest edge of the working electrode and 2 mm below the platinum counter electrode. The surface temperature of the titanium wire in the left hand section was (1587 ± 18) K. Cyclic voltammograms were recorded once the reference electrode and the working counter electrode assembly were positioned in the flame. All scans started at +1 V and scanned at 1 V s^{-1}. See the Supporting Information for full experimental details.

Received: January 10, 2012
Revised: April 26, 2012
Published online: May 15, 2012

Keywords: electrochemistry · gas-phase chemistry · plasma · redox chemistry · voltammetry

[1] a) A. J. Bard, L. R. Faulkner, *Electrochemical Methods: Fundamentals and Applications*, 2nd ed., Wiley, New York, **2000**; b) E. I. Rogers, B. Šljukić, C. Hardacre, R. G. Compton, *J. Chem. Eng. Data* **2009**, *54*, 2049–2053.
[2] a) E. Illenberger, *Chem. Rev.* **1992**, *92*, 1589–1609; b) H. J. Zhai, B. Kiran, L. F. Cui, X. Li, D. A. Dixon, L. S. Wang, *J. Am. Chem. Soc.* **2004**, *126*, 16134–16141; c) J. C. Rienstra-Kiracofe, G. S. Tschumper, H. F. Schaefer, S. Nandi, G. B. Ellison, *Chem. Rev.* **2002**, *102*, 231–282.
[3] a) C. Richmonds, M. Witzke, B. Bartling, S. W. Lee, J. Wainright, C. C. Liu, R. M. Sankaran, *J. Am. Chem. Soc.* **2011**, *133*, 17582–17585; b) S. A. Meiss, M. Rohnke, L. Kienle, S. Z. El Abedin, F. Endres, J. Janek, *ChemPhysChem* **2007**, *8*, 50–53; c) A. Hickling, M. D. Ingram, *Trans. Faraday Soc.* **1964**, *60*, 783–786.
[4] a) M. Vennekamp, J. Janek, *Solid State Ionics* **2001**, *141*, 71–80; b) M. Brettholle, O. Hofft, L. Klarhofer, S. Mathes, W. Maus-Friedrichs, S. Z. El Abedin, S. Krischok, J. Janek, F. Endres, *Phys. Chem. Chem. Phys.* **2010**, *12*, 1750–1755; c) Z. Ogumi, Y. Uchimoto, Z. Takehara, *Adv. Mater.* **1995**, *7*, 323–325.
[5] a) J. Ghoroghchian, F. Sarfarazi, T. Dibble, J. Cassidy, J. J. Smith, A. Russell, G. Dunmore, M. Fleischmann, S. Pons, *Anal. Chem.* **1986**, *58*, 2278–2282; b) M. Krausa, K. Schorb, *J. Electroanal. Chem.* **1999**, *461*, 10–13; c) J. Ghoroghchian, S. Pons, M. Fleischmann, *J. Electroanal. Chem.* **1991**, *317*, 101–108.
[6] a) A. B. Fialkov, *Prog. Energy Combust. Sci.* **1997**, *23*, 399–528; b) J. M. Goodings, J. Z. Guo, A. N. Hayhurst, S. G. Taylor, *Int. J. Mass Spectrom.* **2001**, *206*, 137–151.
[7] B. S. Fialkov, I. A. Larionova, A. B. Fialkov, *Combust. Explos. Shock Waves* **1995**, *31*, 679–684.
[8] J. S. Chang, J. G. Laframboise, *J. Phys. D* **1993**, *26*, 42–48.
[9] G. Berden, R. Peeters, G. Meijer, *Int. Rev. Phys. Chem.* **2000**, *19*, 565–607.
[10] J. M. Goodings, *Abstr. Pap. Am. Chem. Soc.* **1991**, *202*, 201-PHYS.
[11] a) E. Hadzifejzovic, J. A. S. Galiani, D. J. Caruana, *Phys. Chem. Chem. Phys.* **2006**, *8*, 2797–2809; b) E. Hadzifejzovic, J. Stankovic, S. Firth, P. F. McMillan, D. J. Caruana, *Phys. Chem. Chem. Phys.* **2007**, *9*, 5335–5339; c) J. M. Goodings, J. Z. Guo, J. G. Laframboise, *Electrochem. Commun.* **2002**, *4*, 363–369.
[12] D. J. Caruana, S. P. McCormack, *Electrochem. Commun.* **2002**, *4*, 780–786.
[13] The point of zero charge (PZC) is equivalent to the plasma potential in plasma physics. This point describes the potential at which the interface has a net zero capacity, that is, the potential of the electrode is matched to the potential of the medium. This occurs at a potential after the change over from cation current (negative current) to electron current (positive current) according to the Langmuir probe theory and depicted in Figure 1b, and

 © 2012 Wiley-VCH Verlag GmbH & Co. KGaA, Weinheim

can be easily determined from the voltammograms presented in this study. For details see H. F. Calcote, D. E. Jensen, *Adv. Chem. Ser.* **1966**, 291 – 297.
[14] T. Fowowe, PhD thesis, University College London (London), **2011**.
[15] J. A. S. Galiani, E. Hadzifejzovic, R. A. Harvey, D. J. Caruana, *Electrochim. Acta* **2008**, *53*, 3271 – 3278.
[16] a) C. Hoang-Van, O. Zegaoui, *Appl. Catal. A* **1995**, *130*, 89 – 103; b) R. G. Palgrave, I. P. Parkin, *J. Mater. Chem.* **2004**, *14*, 2864 – 2867.
[17] A. K. Vijh, *Mater. Chem. Phys.* **1986**, *14*, 47 – 56.
[18] a) I. R. King, H. F. Calcote, *J. Chem. Phys.* **1955**, *23*, 2203 – 2204; b) C. S. Maclatchy, H. C. L. Smith, *IEEE Trans. Plasma Sci.* **1991**, *19*, 1254 – 1258.
[19] a) M. Abonnenc, L. A. Qiao, B. H. Liu, H. H. Girault, *Annu. Rev. Anal. Chem.* **2010**, *3*, 231 – 254; b) D. Sarantaridis, D. J. Caruana, *Anal. Chem.* **2010**, *82*, 7660 – 7667; c) D. Sarantaridis, C. Hennig, D. J. Caruana, *Chem. Sci.* **2012**, DOI: 10.1039/C2SC20304A.

 © 2012 Wiley-VCH Verlag GmbH & Co. KGaA, Weinheim